Journal of Engineering
journal homepage: www.joe.uobaghdad.edu.iq
Number 8 Volume 26 August 2020

Water Resources and Surveying Engineering

Roughness Effect on Velocity Distribution in Selected Reach of Shatt al-Arab River

Amjed Mohammed Abbas *
College of Engineering, University of Baghdad
E-Mail: ama.eng8286@gmail.com

Prof. Dr. Abdul-Ilah Y. Mohammed
College of Engineering, University of Baghdad
E-Mail: abdulilah.g4@gmail.com

ABSTRACT

Shatt al-Arab is the only navigational artery in Iraq, extending from the city of Qurna to its mouth in the Arabian Gulf at the city of Al-Fao within the governorate of Basrah for a length of approximately 204 km. Its width ranges from 400 m to 2000 m, and its depth ranges from 8 m to 20 m. The southern part of it, 93 km long from Umm al-Rassas Island to Ras al-Bisha, represents the international border between Iraq and Iran, where the Thalweg line represents the border between the two countries, which is the deepest point in the riverbed (according to the 1975 Algiers Agreement). The western bank (the Iraqi side) within the common border of Shatt al-Arab is subject to continuous erosion, which leads to the shifting of the Thalweg line towards Iraqi territory and thus leads to loss of Iraqi land to Iran. Reducing flow velocity along the Iraqi side can lead to reducing or preventing erosion in the river. Increasing the riverbed roughness will reduce the velocity of flow and then reducing the erosion. This principle was adopted in this study to investigate the effect of increasing roughness in a strip along a reach of the riverbed on the distribution of longitudinal velocity in cross-sections at the rest of the selected reach. A reach of Shatt al-Arab with a length of 2500 m, located 34 km north of Fao City, was selected to represent the study area. This reach was simulated by using numerical modeling CFD solver (fluent) with three different roughnesses for an upstream part of the river bed and the velocities compared with the natural (original) roughness of Shatt al-Arab. The results showed an appreciable effect of the increased bed roughness on the velocity distribution and the maximum velocity location by shifting it to the other side.

Keywords: Manning Velocity Distribution; Shatt al-Arab; Fluent.

تأثير الخشونة على توزيع السرعة في جزء محدد من نهر شط العرب

أمجد محمد عباس
كلية الهندسة- جامعة بغداد

أ. د. عبد الاله يونس محمد
كلية الهندسة- جامعة بغداد

الخلاصة

شط العرب هو الشريان الملاحي الوحيد في العراق، ويمتد من مدينة القرنة إلى مصبه في الخليج العربي في مدينة الفاو ضمن محافظة البصرة بطول حوالي 204 كم. يتراوح عرضه من 400 م إلى 2000 م ويتراوح عمقه من 8 م إلى 20 م. يمثل الجزء

*Corresponding author
Peer review under the responsibility of University of Baghdad.
https://doi.org/10.31026/j.eng.2020.08.04

Article received: 22/1/2020
Article accepted:13/3/2020
Article published:1/8/2020

الجنوبي منه ، على بعد 93 كم من جزيرة أم الرصاص إلى رأس البيشا ، الحدود الدولية بين العراق وإيران ، حيث يمثل خط الثالوك الحدود بين البلدين ، وهي أعمق نقطة في مجرى النهر (وفقًا لاتفاقية الجزائر عام 1975). تتعرض الضفة الغربية (الجانب العراقي) داخل الحدود المشتركة لشط العرب إلى تآكل مستمر مما يؤدي إلى تحول خط الثالوك نحو الأراضي العراقية وبالتالي يؤدي إلى فقدان الأراضي العراقية لصالح إيران. يمكن أن يؤدي تقليل سرعة التدفق على طول الجانب العراقي إلى تقليل أو منع التآكل في النهر. تؤدي زيادة خشونة مجرى النهر إلى تقليل سرعة التدفق ومن ثم تقليل التآكل. تم تبني هذا المبدأ في هذه الدراسة للتحقيق في تأثير زيادة الخشونة في شريط على طول مجرى قاع النهر على توزيع السرعة الطولية في المقاطع العرضية في بقية الجزء المحدد. تم اختيار جزء من شط العرب بطول 2500 متر ، ويقع على بعد 34 كم شمال مدينة الفاو ، لتمثيل منطقة الدراسة. تمت محاكاة هذا الامتداد باستخدام النمذجة الرقمية CFD مع ثلاثة خشونات مختلفة لجزء من قاع منطقة الدراسة وتمت مقارنة النتائج مع الحالة الطبيعية لشط العرب (خشونة طبيعية). أظهرت النتائج تأثيرًا ملموسًا لزيادة خشونة جزء من قاع النهر على توزيع السرعة والموقع الأقصى للسرعة من خلال تحويلها إلى الجانب الآخر.

الكلمات الرئيسية: معامل مانغ ، توزيع السرعة ، شط العرب

1. INTRODUCTION

Shatt al-Arab is located in southeastern Iraq within the governorate of Basrah and is approximately 204 km long. The final 93 km of the river forms the international border between Iraq and Iran **(Al-Fartusi, 2013)**. The deepest points along the international border between the two countries configure an imaginary line called (Thalweg Line) according to (**Algiers Convention 1975**).

For along years ago, the Shatt al-Arab River stayed suffers from erosion at the western side (the Iraqi side), which caused gradual encroaching of AL- Thalweg line toward the Iraqi territory. That led to losing the Iraqi territory (Ibrahim **2017)**. One of the methods that can be applied in order to prevent erosion in rivers is reducing the water flow velocity (**Ibrahim-Mageed 2014)**, and in this research, this way can be achieved by increasing the river bed roughness. Because of the difficulties of physical simulation, long time of testing, accuracy results weakness, and scaling problems, a numerical simulation method was used. Shatt al-Arab river problem was numerically simulated by using a commercial CFD solver (FLUENT).

2.DESCRIPTION OF THE STUDY AREA

The study area is a reach of Shatt-al-Arab which is located at 34 km north Al-Fao City which started from the mouth of the Shatt al-Arab to the Arabian Gulf, E=245006, N=3349551, of 2.5 km length between km 60+00 to km 62+500 and 860m width and 11m depth-averaged as shown in **Fig.1**. An area 500m length and 220m width at the reach upstream was allocated from the riverbed to simulate different roughness.

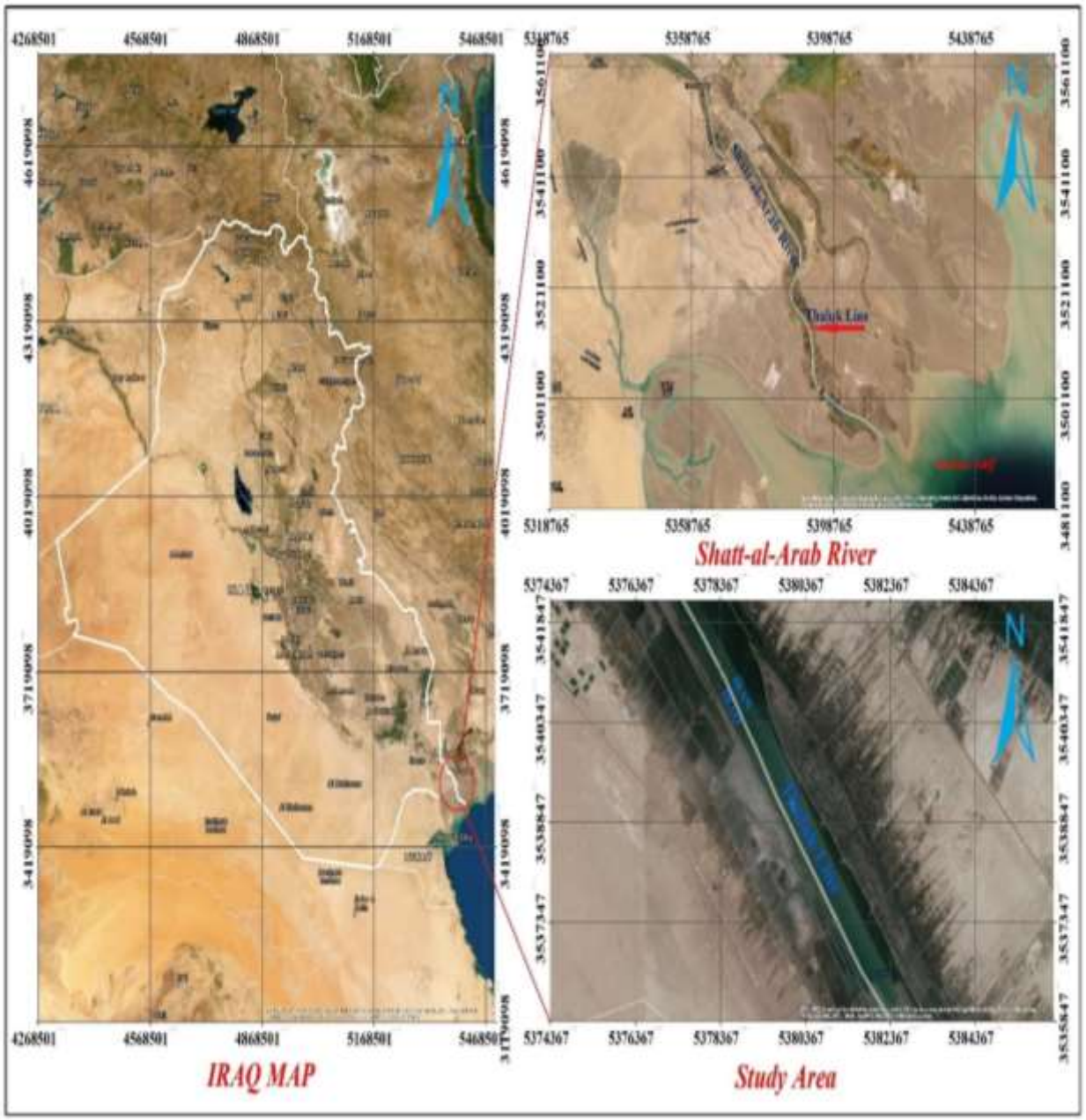

Figure 1. The general layout of the Shatt-al-Arab River, ARC MAP.

3. NUMERICAL SIMULATION

In the current study, different softwares were used to generate a digital model. These softwares were the Civil 3D, Gambit, Space Clam, Hec-Ras, and Ansys Fluent (CFD). The CFD solver FLUENT used in the present study solves the three-dimensional Reynolds-averaged Navier-Stokes equations for incompressible flow. FLUENT solves the governing equations sequentially using the control volume method.

Shatt al-Arab River cross-sections data were provided from the General State of Survey (Ministry of Water Resources). A certain area at upstream of the reach on the Iraqi side was selected to increase the roughness in each case, as shown in **Fig.2**. Four cross-sections (S1, S2, S3, and S4) were selected at 500 m spacing along the reach in which the first section started at a distance of 250 m upstream of the reach to investigate the lateral behavior of the vertical distribution of the longitudinal velocity. At each section, the velocity profiles at three vertical lines (A, B, and C) located at (1/4, 1/2, and 3/4) of the river width started from the

Iraqi side, respectively, as in **Fig.3**. These lines were used to compare the vertical velocity distribution in each case. Four (4) cases were run in the software. The first case (natural conditions) all riverbed has the same roughness height of (0.05 m equivalent to Manning's n of 0.033, according to Stickler's equation (1). In other cases, the natural conditions were maintained, but the roughness height in the designated area was changed to 0.25, 0.75 and 1.25 m (equivalent to Manning's n of 0.033, 0.04, and 0.043) in the (case 2, case 3, and case 4) respectively. The boundary conditions that were used are the inlet condition (mass flow inlet), the water surface condition (atmospheric pressure), the bed and allocated area condition (stationary and non-slip walls), and outlet conditions (both the pressure at the outlet and the constant water surface elevation) were imposed. Furthermore, the Volume of Fluid (VOF) method and Shear Stress Transport (SST) k-ω turbulent model were used in this simulation.

$$n = 0.0132 D_{50}^{1/6} \quad \text{(Stickler's equation)} \qquad (1)$$

Where:
n = Manning's n

D_{50} = roughness height of bed material

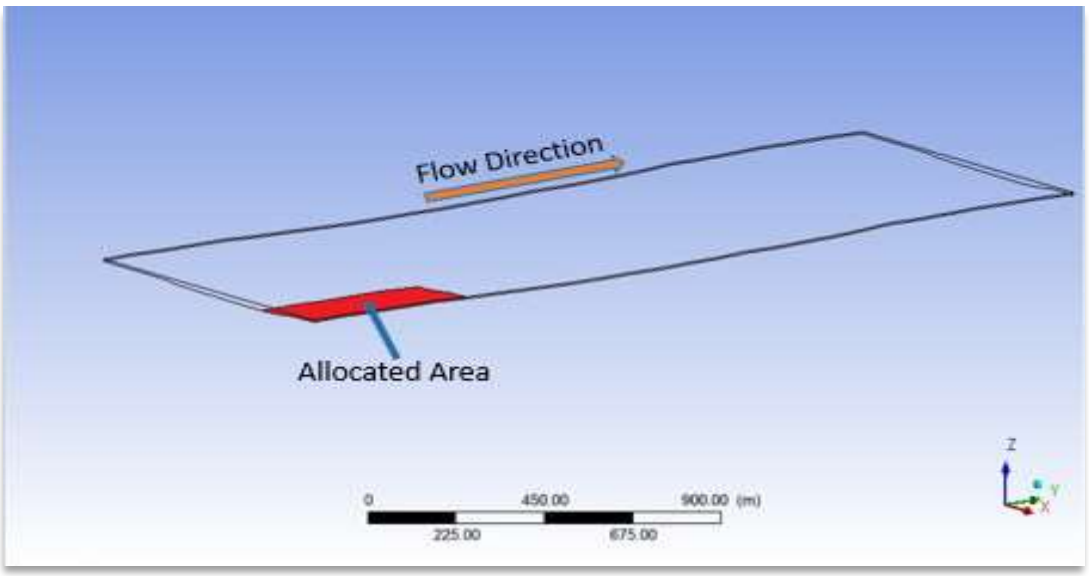

Figure 2. Allocated area of increased roughness in the river reach.

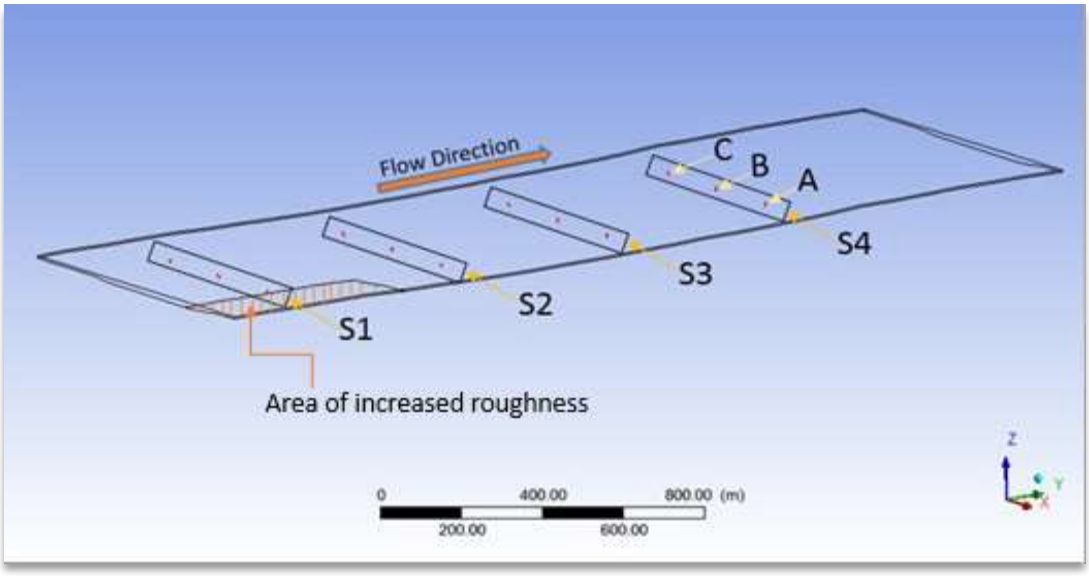

Figure 3. Results points' location at Study Area.

4. RESULTS AND DISCUSSION

Four runs were simulated to investigate the effect of changing bed roughness at the upstream part of the river reach on the longitudinal velocity (v) distribution along the rest reach. Each run represents Manning's n of (0.025, 0.033, 0.04 and 0.043). The results arranged as **Figures (4 to 15)**. In each figure, the vertical distribution of the longitudinal velocity (v) for the four runs was represented. Also, for all lines (A, B, and C) in all sections. **Fig.4** shows that when Manning's n was increased in allocated area to (0.033, 0.04 and 0.043) the average value of the longitudinal velocity at section S1 vertical line A (S1 A) decreased by (5%, 12%, and 25%) for (n=0.033, 0.04 and 0.043) respectively, compared with the natural case (Manning's n =0.025).

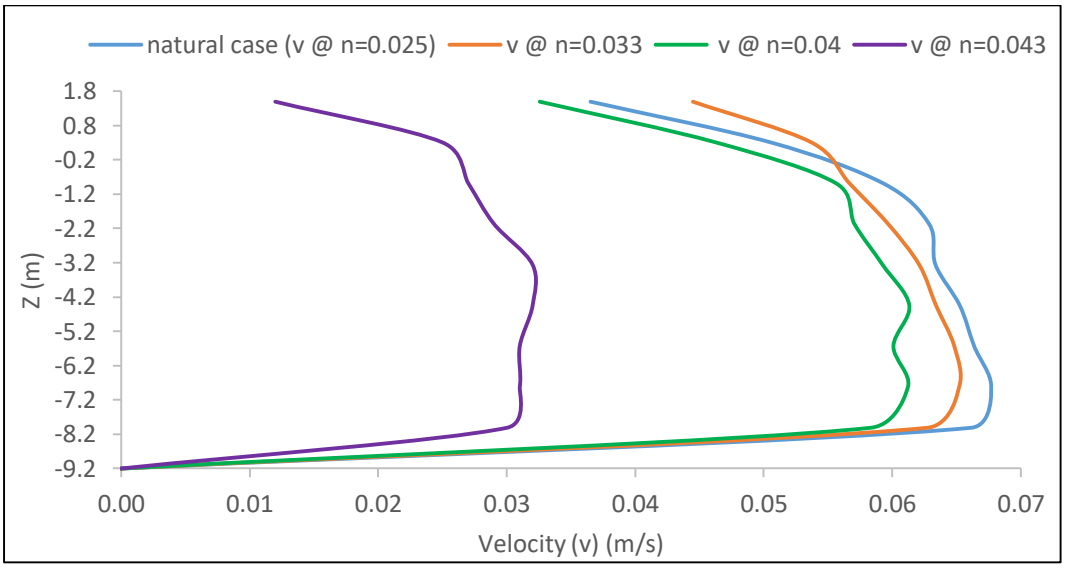

Figure 4. Longitudinal Velocity Distribution at (S1 A).

Fig.5 shows that when Manning's n was increased to (0.033, 0.04 and 0.043) the average value of the longitudinal velocity at (S1 B) increased by (5%, 25% and 34%) for (n=0.033, 0.04 and 0.043) respectively.

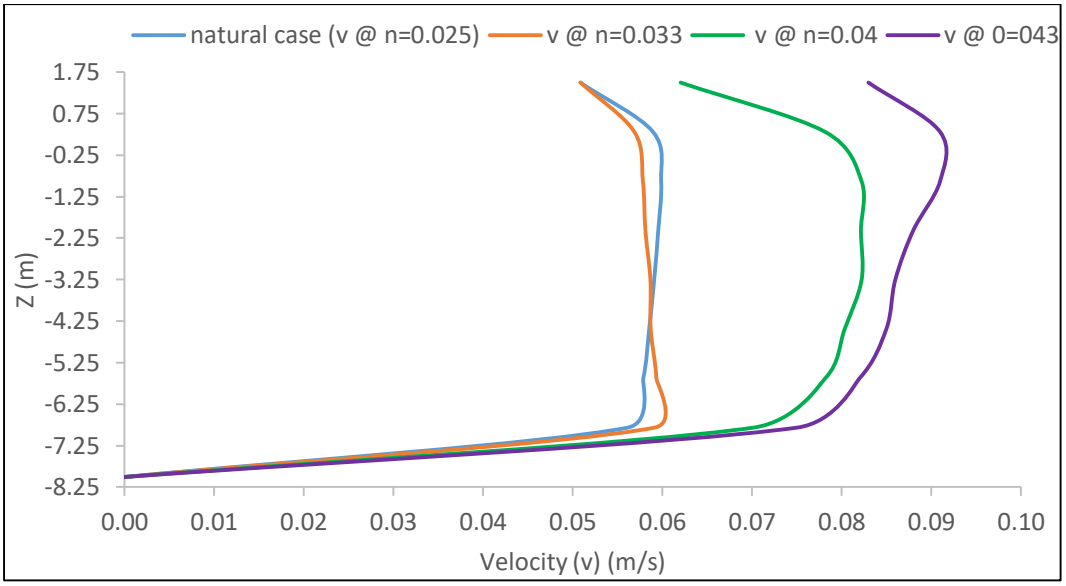

Figure 5. Longitudinal Velocity Distribution at (S1 B).

Fig.6 shows that when Manning's n was increased to (0.033, 0.04 and 0.043) the average value of the longitudinal velocity at (S1 C) increased by (5%, 18% and 20%) for (n=0.033, 0.04 and 0.043) respectively.

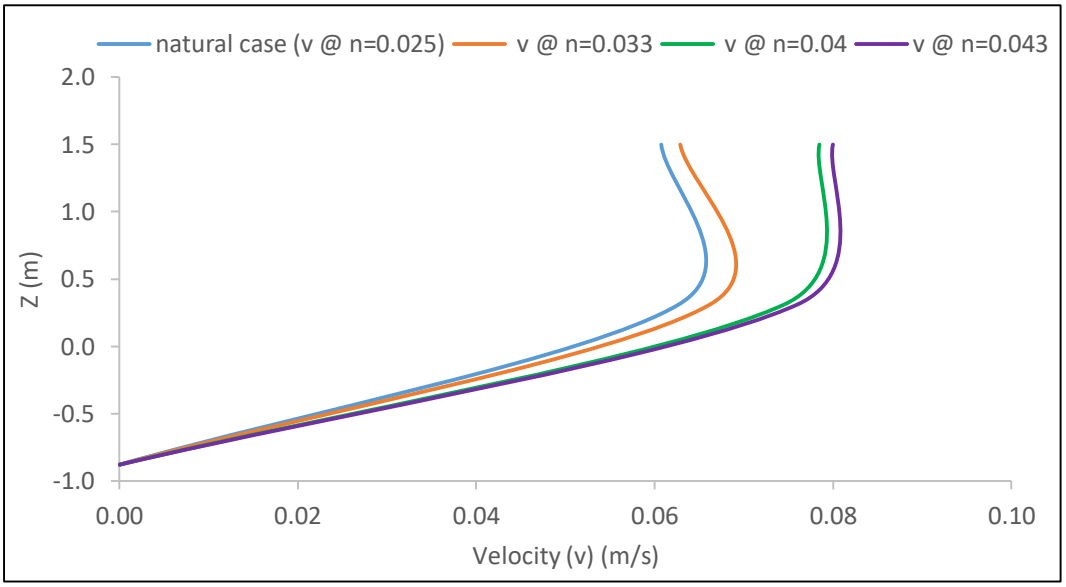

Figure 6. Longitudinal Velocity Distribution at (S1 C).

Fig.7 shows that when Manning's n was increased in allocated area to (0.033, 0.04 and 0.043) the average value of the longitudinal velocity at (S2 A) decreased by (7%, 40%, and 68%) for

(n=0.033, 0.04 and 0.043) respectively, compared with the original case (Manning's n =0.025). Still, in the case of n = 0.043, the velocity direction was in the opposite direction of flow.

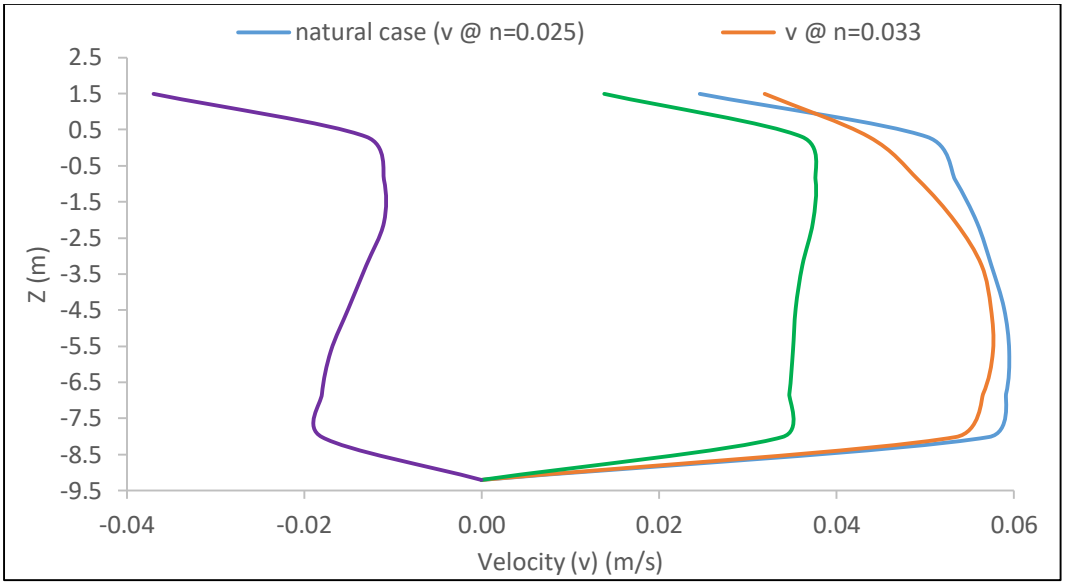

Figure 7. Longitudinal Velocity Distribution at (S2 A).

Fig.8 shows that when Manning's n was increased to (0.033, 0.04, and 0.043) the average value of the longitudinal velocity at (S2 B) increased by (20%, 88%, and 108%) for (n=0.033, 0.04, and 0.043) respectively, compared with the original case.

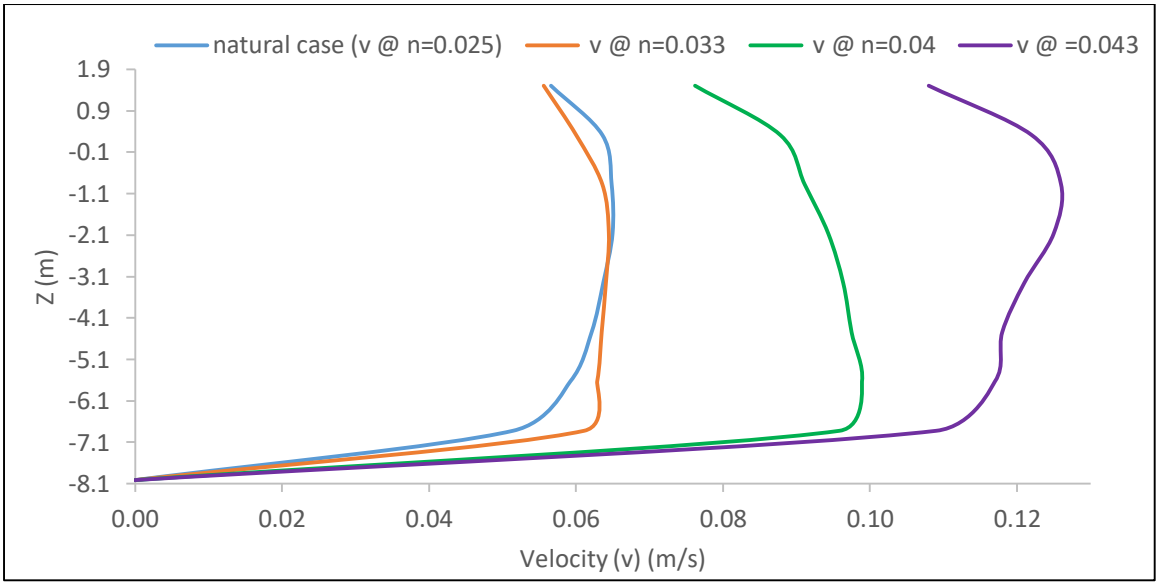

Figure 8. Longitudinal Velocity Distribution at (S2 B).

Fig.9 shows that when Manning's n was increased to (0.033, 0.04, and 0.043) the average value of the longitudinal velocity at (S2 C) increased by (21%, 49%, and 71%) for (n=0.033, 0.04 and 0.043) respectively, compared with the original case.

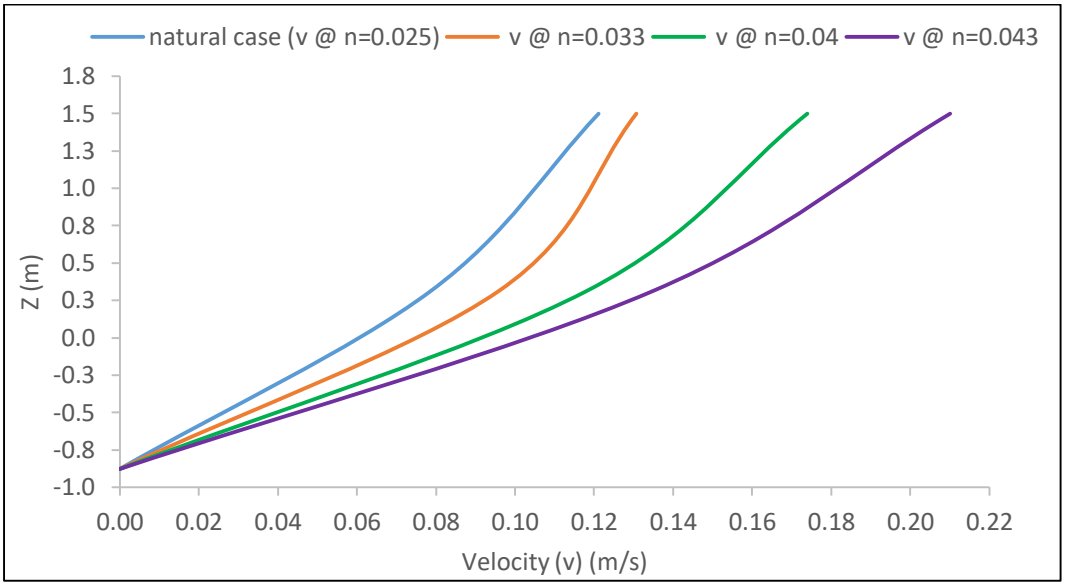

Figure 9. Longitudinal Velocity Distribution at (S2 C).

Fig.10 shows that when Manning's n was increased in allocated area to (0.033, 0.04 and 0.043) the average value of the longitudinal velocity at (S3 A) decreased by (19%, 83%, and 55%) for (n=0.033, 0.04 and 0.043) respectively, compared with the original case (Manning's n =0.025). Still, in the case of n = 0.043, the velocity direction was in the opposite direction of flow.

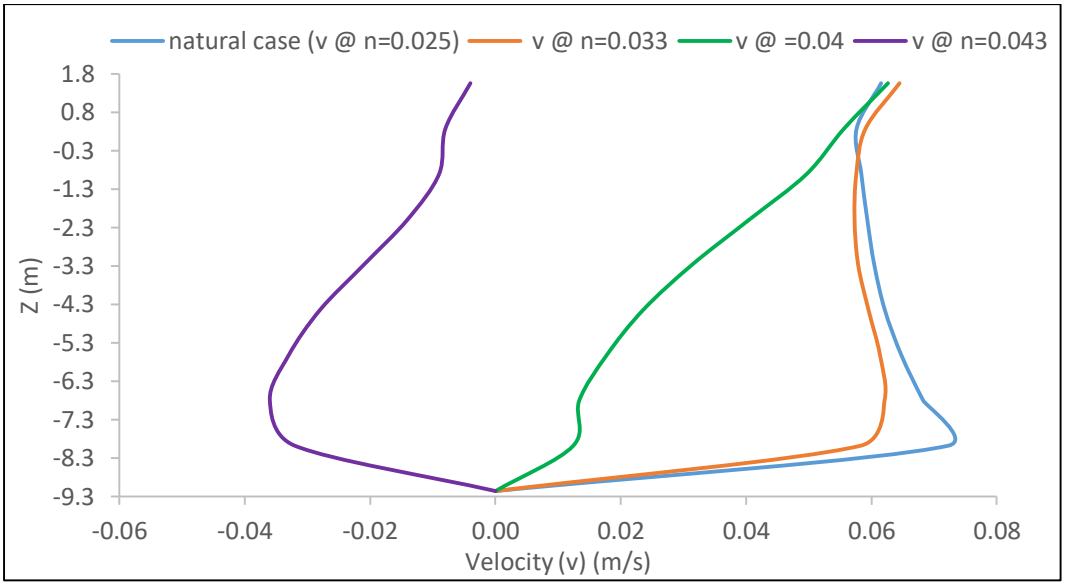

Figure 10. Longitudinal Velocity Distribution at (S3 A).

Fig.11 shows that when Manning's n was increased to (0.033, 0.04 and 0.043) the average value of the longitudinal velocity at (S3 B) increased by (60%, 162%, and 210%) for (n=0.033, 0.04 and 0.043) respectively, compared with the original case.

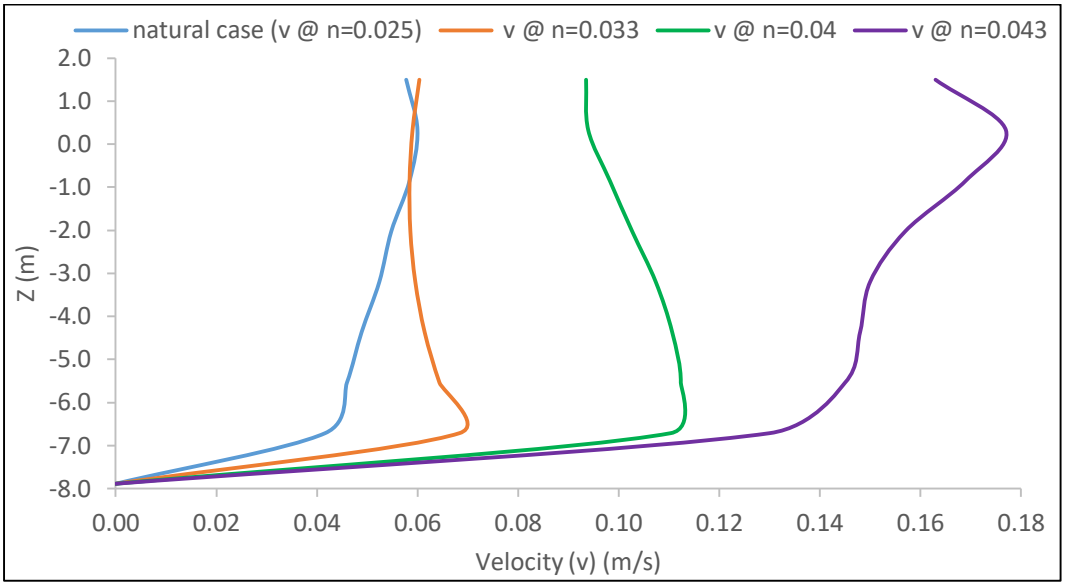

Figure 11. Longitudinal Velocity Distribution at (S3 B).

Fig.12 shows that when Manning's n was increased to (0.033, 0.04, and 0.043) the average value of the longitudinal velocity at (S3 C) increased by (43%, 406%, and 614%) for (n=0.033, 0.04, and 0.043) respectively, compared with the original case.

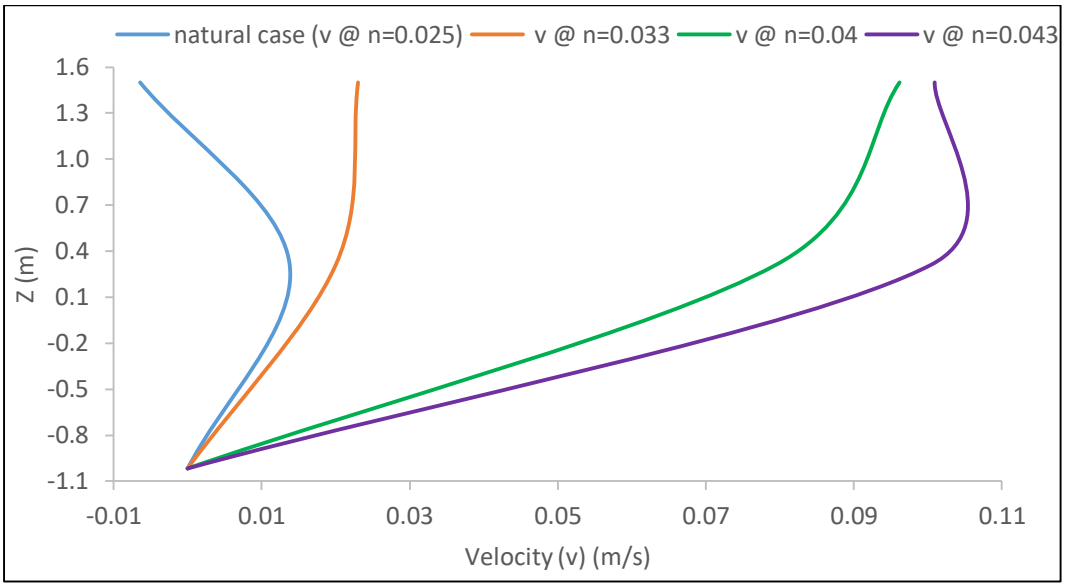

Figure 12. Longitudinal Velocity Distribution at (S3 C).

Fig.13 shows that when Manning's n was increased in the allocated area to (0.033, 0.04, and 0.043). The average value of the longitudinal velocity at (S4 A) decreased by (9%, 90%, and 35%) for (n=0.033, 0.04, and 0.043) respectively, compared with the original case (Manning's n =0.025). Still, in the case of n = 0.043, the velocity direction was in the opposite direction of flow.

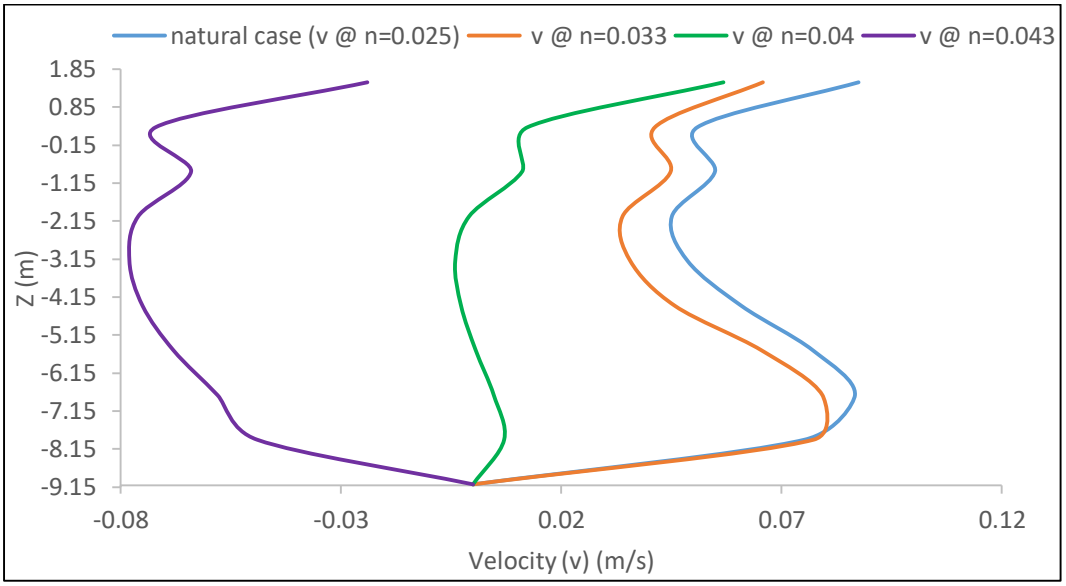

Figure 13. Longitudinal Velocity Distribution at (S4 A).

Fig.14 shows that when Manning's n was increased to (0.033, 0.04, and 0.043) the average value of the longitudinal velocity at (S4 B) increased by (11%, 142%, and 297%) for (n=0.033, 0.04 and 0.043) respectively, compared with the original case.

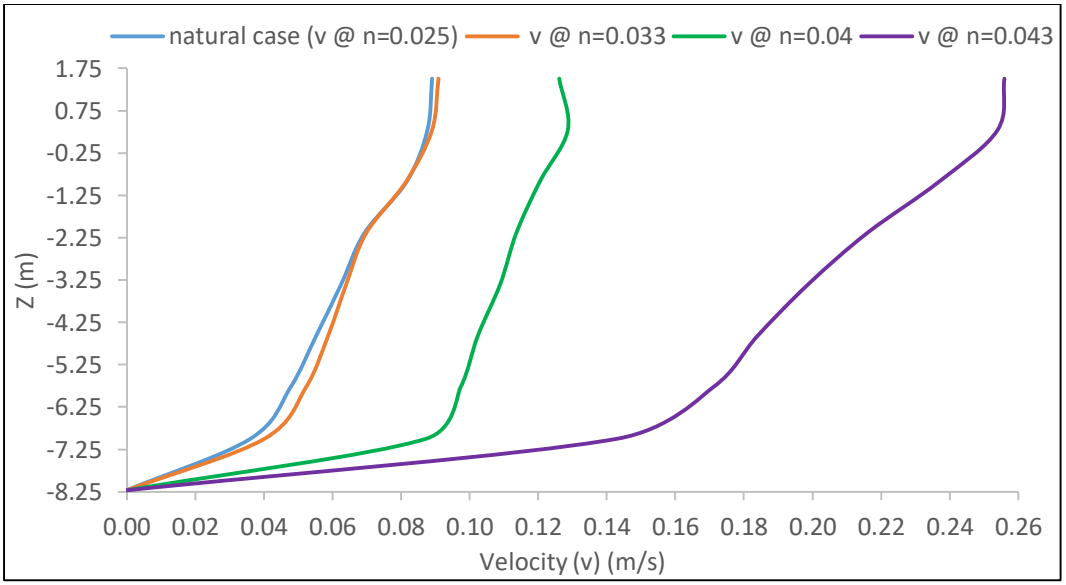

Figure 14. Longitudinal Velocity Distribution at (S4 B).

Fig.15 shows that when Manning's n was increased to (0.033, 0.04, and 0.043) the average value of the longitudinal velocity at (S4 C) increased by (15%, 409%, and 645%) for (n=0.033, 0.04 and 0.043) respectively, compared with the original case.

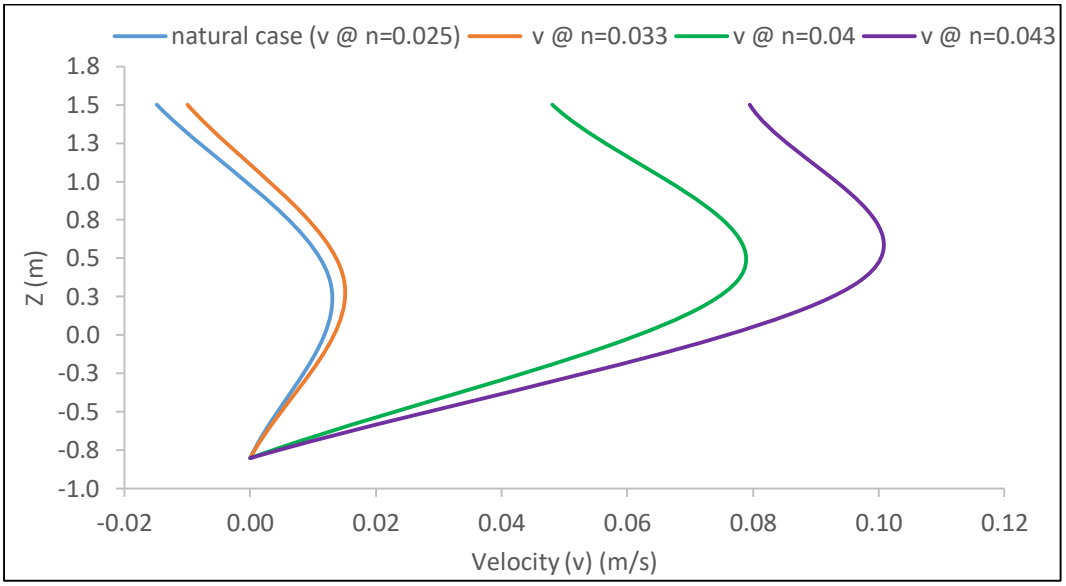

Figure 15. Longitudinal Velocity Distribution at (S4 C).

5. CONCLUSIONS

The simulation results show that when increasing the roughness at the allocated area, the vertical distribution of the longitudinal velocity decreased at the western side and gradually shifted laterally direction to the eastern side. It was observed that the maximum velocity relocated to the middle of the river width. Furthermore, the vertical distribution, the highest velocity, shifted away as increasing bed roughness in the allocated area. These performing is considered a good indication of altering the bed erosion and shoulder erosion at the western side.

REFERENCES

- Al-Fartusi, A. J., Al-Hashemi, N. H., Al-Ta'ai, S. A., 2013, "Hydrodynamic Simulation of the Shatt Al-Arab River". Journal of Basra. Vol. 93, pp. 117-124.
- Ibrahim, S. T., 2017, "Velocity Distribution in a River Cross Section with Variable Roughness". M.Sc. Thesis, College of Engineering, University of Baghdad.
- Ibrahim, M. M., Abdel-Mageed, N. B., 2014, "Effect of Bed Roughness on Flow Characteristics". International Journal of Academic Research. Vol. 6, pp. 169-178.
- Ministry of Water Resources, General State of Survey, Baghdad, Iraq.
- ANSYS Fluent User's Guide, Release 16.1, April 2015.
- R. Shweikani, M. Kousa, and F. Mizban, "The use of phosphogypsum in Syrian cement industry: Radiation dose to public," Ann. Nucl. Energy, vol. 54, pp. 197–201, 2013.
- I. Calin, M. R., Radulescu, and M. A. Calin, 2015. "Measurement and evaluation of natural radioactivity in phosphogypsum in industrial areas from Romania," J. Radioanal. Nucl. Chem., vol. 304, no. 3, pp. 1303–1312.
- R. Perez-Lopez, J. M. Nieto, J. D. de la Rosa, and J. P. Bolivar, 2015. "Environmental tracers for elucidating the weathering process in a phosphogypsum disposal site: Implications for restoration," J. Hydrol., vol. 529, pp. 1313–1323.
- A. J. G. Santos, B. P. Mazzilli, D. I. T. Favaro, and P. S. C. Silva, 2006. "Partitioning of radionuclides and trace elements in phosphogypsum and its source materials based on sequential extraction methods," J. Environ. Radioact., vol. 87, no. 1, pp. 52–61.

- F. Papageorgiou, A. Godelitsas, and T. J. Mertzimekis, 2016. "Environmental impact of phosphogypsum stockpile in remediated Schistos waste site (Piraeus, Greece) using a combination of γ -ray spectrometry with geographic information systems," Env. Monit Assess, vol. 188.

- M. S Al-Masri., Amin Y., 2010." The Use Of Biosorbents For Heavy Metals Removal From Aqueous Media", Syrian Arab Republic Atomic Energy Commission.

- S.K Gunatilake, 2015. " Methods of Removing Heavy Metals from Industrial Wastewater", Journal of Multidisciplinary Engineering Science Studies Vol. 1, pp.12-18.

- A. Moslehyani, O. M. Nasser, R. Junin, E. Halakoo, A.F. Ismail, 2013. "Polyethersulfone Ultrafiltration Membrane for Oil-in-Water Emulsion Separation", International Conference on Membrane Science and Technology.

- Nasrul Arahman, 2014" Modification of the Morphology of the Poly(ether sulfone) Membrane Prepared by Dry Phase Inversion Technique", International Journal of Applied Engineering Research, Vol.9, No. 21, pp. 10453-10462.

- Bjarne Nicolaisen,"Developments in Membrane Technology for Water Treatment", Desalination, Vol.153, pp355–360, 2003.

- Baker, R. W. ,Membrane Technology and Application. 3rd Edition. John Wiley and Sons Ltd., 2012.

- Zhou, W. and L. Song, 2005."Experimental Study of Water and Salt Fluxes Through Reverse Osmosis Membranes", Environment Science Technology. 39: pp3382–3387.

- Ahmed H. Algureiri and Yossor R. Abdulmajeed, 2016. " Removal of Heavy Metals from Industrial Wastewater by Using RO Membrane ", Iraqi Journal of Chemical and Petroleum Engineering, Vol.17, No.4, pp. 125- 136.

- Arkhangelsky, E., V. Gitis., 2008 "Effect of Transmembrane Pressure on Rejection of Viruses by Ultrafiltration Membranes", Separation and Purification Technology, Vol. 62, No.3, pp 619–628.

- Chuyang Y. Tang, Q. Shiang Fu, Craig S. Criddle, and James O. Leckie, 2008. "Effect of Flux (Transmembrane Pressure) and Membrane Properties on Fouling and Rejection of Reverse Osmosis and Nanofiltration Membranes Treating Perfluorooctane Sulfonate Containing Wastewater", Environ. Sci. Technol. 41, pp 2008–2014.

- Jyothi, Vignesh Nayak, Mahesh Padaki, R. Geetha Balakrishna, A.F. Ismail, 2014. " The effect of UV irradiation on PSF/TiO_2 mixed matrix membrane for chromium rejection", Desalination, Vol. 354, pp.189–199.

- Irfana Moideen K, Arun M. Isloor, A.F. Ismail, Abdulrahman Obaid, and Hoong Kun Fun, 2015. ”Fabrication and characterization of new PSF/PPSU UF blend membrane for heavy metal rejection”, Desalination and Water Treatment, p.1-10.

- Sofía Riaño and Koen Binnemans, 2015. ”Extraction and separation of neodymium and dysprosium from used NdFeB magnets: an application of ionic liquids in solvent extraction towards the recycling of magnets” The Royal Society of Chemistry, Green Chem., Nol.17, p.2931–2942.

- Suad Abdulmuttaleb Mohammed, Areej Dalaf Abbas, Laith Salim Sabri, 2014. ” Effect of Operating Conditions on Reverse Osmosis (RO) Membrane Performanceincreasing Journal of Engineering, Number 12, Volume 20.